Roles of Salt and Conformation in the Biological and Physicochemical Behavior of Protegrin-1 and Designed Analogues: Correlation of Antimicrobial, Hemolytic, and Lipid Bilayer-Perturbing Activities†

Jonathan R. Lai,‡,# Raquel F. Epand,§,# Bernard Weisblum,|| Richard M. Epand,*,§ and Samuel H. Gellman*,‡,⊥

Graduate Program in Biophysics and Departments of Chemistry and Pharmacology, University of Wisconsin, Madison, Wisconsin 53706, and Department of Biochemistry and Biomedical Sciences, McMaster University Health Sciences Center, Hamilton, Ontario, Canada L8N 3Z5

Received August 28, 2006; Revised Manuscript Received October 6, 2006

ABSTRACT: Protegrins are short (16−18 residues) cationic peptides from porcine leukocytes that display potent, broad-spectrum antimicrobial activity. Protegrin-1 (PG-1), one of five natural homologues, adopts a rigid β-hairpin structure that is stabilized by two disulfide bonds. We have previously employed the principles of β-hairpin design to develop PG-1 variants that lack disulfide bonds but nevertheless display potent antimicrobial activity [Lai, J. R., Huck, B. R., Weisblum, B., and Gellman, S. H. (2002) *Biochemistry 41*, 12835−12842.]. The activity of these disulfide-free variants, however, is attenuated in the presence of salt, and the activity of PG-1 itself is not. Salt-induced inactivation of host-defense peptides, such as human defensins, is thought to be important in some pathological situations (e.g., cystic fibrosis), and the variation in salt-sensitivity among our PG-1 analogues offers a model system with which to explore the origins of these salt effects. We find that the variations in antimicrobial activity among our peptides are correlated with the folding propensities of these molecules and with the extent to which the peptides induce leakage of contents from synthetic liposomes. Comparable correlations were observed between folding and hemolytic activity. The extent to which added salt reduces antimicrobial activity parallels salt effects on vesicle perturbation, which suggests that the biological effects of high salt concentrations arise from modulation of peptide−membrane interactions.

The protegrins are short (16−18 residues) cationic peptides from porcine leukocytes that display potent, broad-spectrum antimicrobial activity (*1*−*5*). Five natural protegrin homologues have been identified to date (PG-1[1] through −5; Figure 1A). All have a high content of arginine, an amidated C-terminus, and cysteine residues at positions 6, 8, 13, and

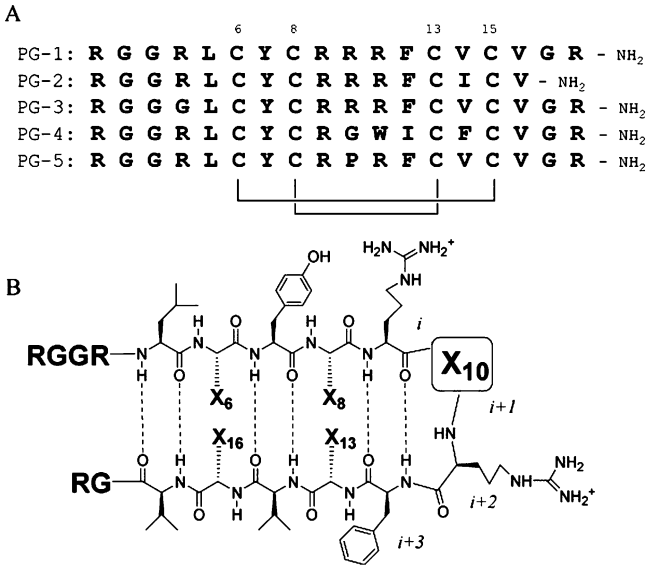

FIGURE 1: (A) Sequences and disulfide-bonding arrangement of protegrins PG-1 through −5. (B) General β-hairpin schematic of the peptides examined in this study. The sites of variation are indicated by X_6, X_8, X_{10}, X_{13} and X_{16}.

15 that are disulfide-bonded in the arrangement Cys_6-Cys_{15} and Cys_8-Cys_{13}. PG-1 (sequence $^+NH_3$−RGGRLC_6YC_8-RRRFC_{13}VC_{15}VGR−amide) has a rigid antiparallel β-hairpin structure with the charged residues clustered at either end of the β-hairpin and a central hydrophobic core (a general

† This research was supported by the National Institutes of Health (GM 61238 to S.H.G.) and the Canadian Institutes of Health Research (MT-7654 to R.M.E.). J.R.L was supported in part by a PGS B scholarship from the Natural Sciences and Engineering Research Council (NSERC) of Canada.

* To whom correspondence should be addressed. Phone: (905) 525-9140 ext. 22073 (R.M.E.), (608) 262-3303 (S.H.G.). Fax: (905) 521-1397 (R.M.E.), (608) 265-4534 (S.H.G.). E-mail: epand@mcmaster.ca (R.M.E.), gellman@chem.wisc.edu (S.H.G.).

‡ Graduate Program in Biophysics, University of Wisconsin.

§ Department of Biochemistry and Biomedical Sciences, McMaster University.

|| Department of Pharmacology, University of Wisconsin.

⊥ Department of Chemistry, University of Wisconsin.

# These authors contributed equally to this work.

[1] Abbreviations: PG-1, protegrin-1; NMR, nuclear magnetic resonance; CF, cystic fibrosis; MALDI−TOF, matrix-assisted laser desorption/ionization−time-of-flight; CD, circular dichroism; DOPE, dioleoylphosphatidylethanolamine; DOPC, dioleoylphosphatidylcholine; DOPG, dioleoylphosphatidylglycerol; DOPS, dioleoylphosphatidylserine; py-12-PC, 1-lauroyl-2-(1′pyrenebutyroyl)-*sn*-glycero-3-phosphocholine; LUV, large unilamellar vesicle; SUV, small or sonicated unilamellar vesicle; ANTS, 8-aminonaphthalene-1,3,6-trisulfonic acid; DPX, *p*-xylene-bis-pyridinium bromide; MIC, minimum inhibitory concentration; L/P, lipid to peptide molar ratio; HPLC, high-performance liquid chromatography; N-Rh-PE, 1,2-dioleoyl-3-*N*-phosphoethanolamine-*N*-(lissamine rhodamine B-sulfonyl); ITC, isothermal titration calorimetry.

10.1021/bi0617759 CCC: $33.50
Published on Web 12/01/2006

β-hairpin schematic for the peptides studied in this work is shown in Figure 1B) (*6*, *7*). Studies with PG-1 sequence variants have demonstrated that this overall topology (cation/hydrophobic/cation architecture) is required for antimicrobial activity (*8*). The protegrins are potential prototypes for the development of new clinical anti-infective agents (*8*), and it is therefore important to understand how peptide sequence and conformational propensity are related to biological activity.

The rigidity of the PG-1 β-hairpin arises from the two internal disulfide bonds, which are important for antimicrobial activity (*8*−*10*). Mutation of the four cysteines to alanines or derivatization of the cysteinyl thiols to block disulfide bond formation results in analogues that are inactive (*8*−*10*). However, the cysteines can be eliminated with retention of native PG-1-like activity if the peptide is backbone-cyclized (*11*). PG-1 variants containing only one of the two native disulfide bonds retain considerable antimicrobial activity (*9*). Hong and co-workers have suggested that conformational rigidity plays a more significant role in activity than does overall charge (*12*). We and Robinson et al. have demonstrated that active analogues of PG-1 lacking disulfide bonds can be designed using a D-proline-containing β-hairpin-promoting turn to stabilize a folded conformation of the peptide (*13*, *14*).

PG-1 is monomeric in aqueous solution (*6*), but NMR experiments in the presence of perdeuterated phospholipids suggest that the peptide dimerizes in a head-to-tail fashion in the membrane (*15*). These findings are consistent with biophysical studies that show that protegrins form ion-conducting pores in membranes (*16*), implying an antimicrobial mechanism for PG-1 that is similar to the mechanism postulated for the human defensin HNP-3 (*17*). Diffraction studies indicate that, at least at low temperature and low hydration, PG-1 can form ordered arrays of pore-like structures in membranous environments (*18*). Recent solid-state NMR studies have provided insight on the orientation of PG-1 when inserted into a bilayer (*19*). The tendency of protegrins to aggregate and insert into a bilayer depends on the nature of the lipid and the concentration of peptide at the membrane surface (*20*). The interaction of PG-1 with bilayers is modulated by the lipid composition, with the peptide inserting more deeply into membranes containing anionic lipids such as lipid A, a component of the outer membrane of Gram-negative bacteria, relative to membranes containing only zwitterionic lipids (*21*).

As with other cationic antimicrobial peptides, PG-1 displays selectivity for disruption of bacterial membranes over mammalian membranes (*1*−*5*). This membrane specificity has its roots in charge−charge interactions. The outer leaflet of bacterial membranes contains a higher population of anionic headgroups than does the outer leaflet of mammalian membranes. Thus, bacteria present an anionic outer surface to the extracellular environment, which allows the cationic antimicrobial peptides to distinguish bacteria from mammalian cells (which have a more neutral outer leaflet lipid composition). The chemical structures of several common anionic and zwitterionic phospholipids (including those used in the current study) are shown in Chart 1.

Protegrins have received much attention as potential therapeutic agents for disorders such as cystic fibrosis (CF) because their antibacterial activity is not diminished at high

Chart 1: General Structure of Phospholipids and Common Headgroups

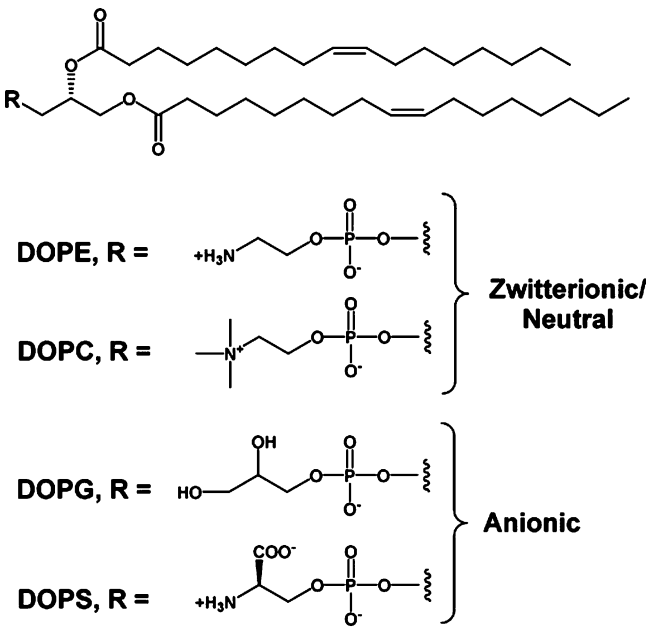

salt concentrations (*9*). This salt-insensitivity contrasts with the behavior of human β-defensins (the natural defense molecules that are secreted by the epithelial cells that line the lung). The antimicrobial potencies of β-defensins are dramatically reduced at >100 mM NaCl (*22*, *23*). It has been proposed that the elevated NaCl concentration in the airway mucus of CF patients compromises the first-line defense against bacterial invaders (by inactivating the defensins), thereby leaving CF patients highly susceptible to opportunistic infection of the airway (*22*, *23*). Although the basis for the inactivation of defensins under these conditions is not known, several reports have suggested that the reduction in defensin potency is due to conformational destabilization under high salt conditions (*23*−*25*). There is no high-resolution structural evidence to support this hypothesis, however. The salt-insensitive activity of PG-1 and analogues has resulted in exploration of these peptides as potential aerosol treatments for CF and oral mucositis (*26*).

In the current study, we explore the relationship between the biological activity of several designed PG-1 analogues and their interaction with synthetic lipid bilayers. This work builds upon an earlier study, in which we used principles of β-hairpin design to engineer a series of PG-1 analogues with variable folding propensities (*13*). Here, we use this control over molecular conformation, exerted by appropriate choice of residues in the turn and β-strand regions, to examine relationships among antimicrobial activity, hemolysis activity, and perturbation of synthetic lipid bilayers. The availability of a peptide series with graded folding propensities and established structure−function correlations (Table 1) has allowed us to examine the influence of varying salt concentrations on peptide−bilayer interactions and antimicrobial activity. PG-1 is known to be fully active in the presence of high salt concentrations (*8*, *9*), but we find that salt-induced diminution of antimicrobial activity becomes increasingly pronounced among PG-1 analogues as folding propensity decreases. This biological trend is mirrored by a physicochemical trend: decreasing β-hairpin propensity leads to decreasing membrane perturbation at higher salt concentra-

Table 1: Peptide Sequences

Peptide[a]	Sequence[b]
PG-1[c]	RGGRL **C** Y **C** RR RF **C** V **C** VGR
TTpTT	RGGRL **T** Y **T** Rp RF **T** V **T** VGR
TTp*TT	RGGRL **V** Y **T** Rp*RF **T** V **I** VGR
CTpTC	RGGRL **C** Y **T** Rp RF **T** V **C** VGR
TTPTT	RGGRL **T** Y **T** RP RF **T** V **T** VGR

[a] All peptides synthesized as C-terminal amides and free N-terminal amines. [b] Sites of variation among peptides are emblazoned in bold. [c] Disulfide cross-links are Cys_6-Cys_{15} and Cys_8-Cys_{13}.

tions. These results suggest that salt effects observed among host−defense peptides and their synthetic analogues arise from alterations in peptide−membrane interactions. The following protegrin analogues were studied in this paper: TTpTT, TTp*TT, CTpTC, and TTPTT, the sequences of which are presented in Table 1.

MATERIALS AND METHODS

Materials. Oregon Green dextran 10 kDa conjugate was purchased from Molecular Probes (Eugene, OR). All other lipids were purchased from Avanti Polar Lipids (Alabaster, AL). Amino acid monomers with appropriate protecting groups for peptide synthesis were purchased from Novabiochem (San Diego, CA). Melittin (for hemolysis assays) was purchased from Sigma (St. Louis, MO).

Peptide Synthesis and Purification. PG-1 and analogues were prepared as previously described using standard 9-fluorenylmethoxycarbonyl (Fmoc) chemistry on a solid support (*13*; the synthesis of γ-(*S*)-amino-D-proline is also described in this reference). All peptides were obtained in good yield. Following HPLC purification, peptides were generally >95% pure as judged by analytical HPLC. Molecular weights observed by MALDI−TOF were in good agreement with the expected peptide masses (not shown).

NMR. Samples for ^{1}H NMR analysis were prepared by dissolving the purified peptides to 1−5 mM in 9:1 H_2O/D_2O containing 40 mM CD_3COOH/CD_3COONa, pH 3.8 (uncorrected). All spectra were recorded on a Varian INOVA 600 MHz spectrometer at 24 °C. Water suppression was achieved either by the Watergate method (*27*) or by selective irradiation. TOCSY (*28*), ROESY (*29*), and NOESY (*30*) data were acquired with a 7 kHz spectral window, a 1 s recycle delay, and mixing times of 80, 200, and 200 ms, respectively. Typical 2-D data sets consisted of 500−600 free induction decay (FID) increments of 16−24 transients each (corresponding to 1938−3874 data points in f_2). Data were processed with Varian VNMR software and referenced to internal 2-(trimethylsilyl)-1-propanesulfonic acid. Spin system assignments were achieved by standard methods (*31*). NMR α-proton chemical shift data for TTpTT (see Table 1) were originally reported in ref 13.

Antimicrobial Assays. Bacteriostatic potency of the peptides was determined in brain heart infusion (BHI) broth containing an additional 300 mM NaCl against several organisms: *Escherichia coli* JM109 (*32*), *Bacillus subtilis* BR151 (*33*), penicillin-resistant *Staphylococcus aureus* 1206 (*34*), and vancomycin-resistant *Enterococcus faecium* A634 (*35*). The purified peptides were dissolved in water to 2 mg/mL (based on the dry weight of the peptide as TFA salts). A 2-fold dilution series for each peptide was then prepared in sterile 96-well Falcon microtiter plates in sterile water. To each well was then added 50 μL of a freshly prepared 10^6 cfu/mL bacterial suspension in 2 × (BHI + 300 mM NaCl) (the total well volume was 100 μL, and the final supplemental NaCl concentration was 300 mM), and the plates were incubated at 37 °C for 6 h. The MIC was defined as the lowest peptide concentration required for complete inhibition of growth, as determined by the optical density (OD) at 590 or 650 nm. The values listed in Table 2 were from two independent experiments, each performed in duplicate. The error associated with the MIC measurement is ±2-fold. BHI broth contains 5 g/L NaCl (~90 mM), and therefore the total salt concentrations for the BHI, BHI + 150 mM NaCl, and BHI + 300 mM NaCl MIC determinations are approximately 90, 240, and 390 mM, respectively. Control experiments indicated that the additional salt in the BHI broth does not significantly affect bacterial growth (not shown). The MICs in BHI and BHI + 150 mM NaCl have been previously determined (*13*).

Hemolysis. 2-Fold peptide serial dilution series were prepared from 2 mg/mL stock solutions in sterile 96-well Falcon microtiter plates in Tris-buffered saline (TBS, 10 mM Tris, 150 mM NaCl, pH 7.2). Freshly-drawn human red blood cells (hRBC, type A) were pelleted and resuspended in TBS several times until a colorless supernatant was observed. A 1% (v/v) cell suspension of the washed hRBCs was prepared in TBS, and 80 μL of this solution was added to each well (the total well volume was 100 μL). The plates were then incubated at 37 °C for 1 h, and then centrifuged at 3500 rpm for 5 min. The supernatant was diluted with 80 μL of TBS, and the amount of hemoglobin in each well was determined by OD_{405}. Melittin was included as a positive control. The data were normalized for % hemolysis using the OD_{405} at high melittin concentration as the 100% reference value, and the OD_{405} of TBS containing no peptide as the 0% reference value. Two independent experiments, each performed in duplicate, yielded similar results.

Preparation of Large Unilamellar Vesicles (LUVs). Lipids were dissolved in chloroform/methanol, 2:1 (v/v) at the desired lipid molar ratio. The lipid was then deposited as a film on the wall of a glass test tube by solvent evaporation with nitrogen. Final traces of solvent were removed for 2−3 h in an evacuated chamber. The lipid films were suspended in the appropriate buffer by vortexing at room temperature to form multilamellar vesicles. The lipid suspensions were further processed with 5 cycles of freezing and thawing, followed by 10 passes through two stacked 0.1 μm polycarbonate filters (Nucleopore Filtration Products, Pleasanton, CA) in a barrel extruder (Lipex Biomembranes, Vancouver, BC) at room temperature. LUVs were stored on ice and used within a short time after preparation.

Liposomal ANTS/DPX Leakage Studies. Aqueous content leakage from liposomes was determined using the ANTS/DPX assay (*36*). Lipid films were hydrated with 12.5 mM 8-aminonaphthalene-1,3,6-trisulfonic acid (ANTS) and 45 mM *p*-xylene-bis-pyridinium bromide (DPX) in 10 mM HEPES, pH 7.4 (the chemical structures of the small molecule dyes are shown in Chart 2). The osmolarity of this solution was adjusted with NaCl to be equal to that of the assay buffer (10 mM HEPES, 0.1 mM EDTA, pH 7.4), as measured with a cryo-osmometer (Advanced Model 3MOplus Micro-Osmometer, Advanced Instruments Inc., Norwood,

Table 2: Minimal Inhibitory Concentrations (μg/mL)

peptide	*E. coli*	*B. Subtilis*	*S. Aureus*[a]	*E. faecium*[b]	ref
BHI					
PG-1	6.3	3.1	12.5	3.1	13
TTpTT	6.3	25	50	12.5−25	13
TTp*TT	3.1	12.5	25	12.5	13
CTpTC	6.3	3.1	12.5	3.1	13
TTPTT	100	200	>200	>200	13
BHI + 300 mM NaCl					
PG-1	6.3	6.3	12.5	3.1	this work
TTpTT	50−100	50−100	>200	200	this work
TTp*TT	12.5	25−50	100	>200	this work
CTpTC	6.3	6.3−12.5	25	25	this work

[a] A penicillin-resistant strain was used. [b] A vancomycin-resistant strain was used.

Chart 2: Chemical Structures of ANTS and DPX

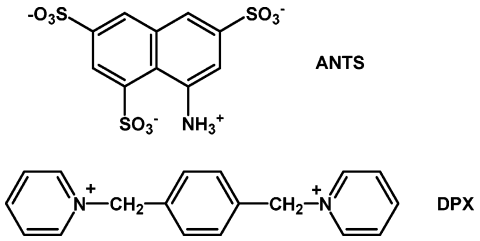

MA). LUVs of 0.1 μm diameter were prepared by extrusion, as described above. After passage through a 2.5 × 20 cm column of Sephadex G-75, the void volume fractions were collected and the phospholipid concentration was determined by phosphate analysis using the method of Ames (*37*). The fluorescence measurements were performed in 2 mL of buffer in a quartz cuvette equilibrated at 37 °C with stirring. Aliquots of LUVs were added to the cuvette, and the fluorescence was recorded as a function of time using an excitation wavelength of 360 nm and an emission wavelength of 530 nm with 8 nm bandwidths. A 500 nm cutoff filter was placed in the emission path. Peptide in buffer was added to the lipid vesicles in the cuvette, and the fluorescence was monitored over time. At the end of each experiment, the value for 100% release was obtained by adding 20 μL of a 10% Triton X-100 solution to the cuvette. Experiments were performed in duplicate; both replicates were in good agreement. Batches of LUVs prepared on different days retained the same order of potentiation within the peptide series but varied in absolute values.

Leakage Assays with Liposomes Entrapping Oregon Green Dextran 10 kD Conjugate by Antibody Quenching. A previously reported procedure (*38*) was modified for this assay. Lipid films were prepared containing 0.02 mol % N−Rh−PE to visualize the liposomes during separation by gel filtration. Lipid films were hydrated with a solution of Oregon Green−dextran 10 kDa conjugate in phosphate-buffered saline (PBS, 10 mM phosphate, 150 mM NaCl) at pH 7.4. The suspensions were vortexed and subjected to five cycles of freeze−thaw, and 100 nm diameter LUVs were prepared by extrusion. The liposomes were passed through a 1 × 40 cm Sepharose 4B-CL gel filtration column, eluted with phosphate-buffered saline (PBS) at pH 7.4 that had been adjusted to be equiosmolar. The liposomes were collected from the column in the void volume. The maximum absorbance of N−Rh−PE at 557 nm was used for quantification of the liposomes. Fluorescence measurements were performed at 37 °C using an SLM Aminco Bowman Series II spectrofluorometer in siliconized round glass cuvettes containing 2 mL of buffer with magnetic stirring. Excitation was achieved at 488 nm and emission monitored at 528 nm with an 8 nm bandpass. LUVs were added to the buffer, and after a baseline was established, peptide solution was added. The fluorescence was monitored for 20 s, and then a solution containing antibody was added in order to quench the fluorescence of the probe that had leaked out of the liposome. At the end of the experiment, an aliquot of 20% Lubrol-PX (0.1% final concentration) was added to obtain 100% dextran release. Light scattering monitored by absorbance at 450 nm and quasi-elastic light scattering (QUELS) demonstrated that increasing salt concentrations did not induce aggregation of LUVs in the presence of TTpTT, TTp*TT, or TTPTT. Therefore, the vesicles remain ∼100 nm in diameter in the presence of these peptides.

Transbilayer Lipid Diffusion. The rate of transbilayer lipid diffusion (flip-flop) was measured using the method described by Müller et al. (*39*). The assay is based on detection of the dilution of a pyrene probe, 1-lauroyl-2-(1′-pyrenebutyroyl)-*sn*-glycero-3-phosphocholine (py-12-PC), as a result of transbilayer diffusion. The probe stock solution was prepared by dissolving py-12-PC in ethanol, then adding the solution to PBS, pH 7.2 (the final ethanol concentration was 5% (v/v)). An aliquot of this stock solution of probe was then added to 20 μM LUV of DOPC/DOPG (7:3) in PBS, pH 7.2, in a quartz cuvette containing 2 mL of buffer. An amount of probe was added to partition only into the outer monolayer at a concentration of 5 mol % of the total lipid or 10 mol % of the outer monolayer. The emission intensities of pyrene for the excimer and for the monomer fluorescence were continuously measured at two different wavelengths, and the ratio of these intensities was recorded as a function of time. Peptides were added to obtain a peptide/lipid ratio (P/L) of 0.1. An excitation wavelength of 344 nm was used with 4 nm bandwidths. The fluorescence of the monomeric form of the probe was measured at an emission wavelength of 395 nm and at 477 nm for the excimer. Controls without the addition of peptides showed no change in fluorescence emission, indicating a slow basal rate of flip-flop. When flip-flop occurs in the presence of peptides, there is a reduction in the excimer/monomer ratio because of the dilution of the probe from one monolayer to two. Controls for fluorescence effects that were independent of flip-flop were also performed using symmetrically labeled LUVs. These symmetrically labeled LUVs were prepared by extrusion, as described above, with the pyrene-labeled lipids mixed with the other lipids in organic solvent prior to making the lipid film and

Chart 3: D-Proline and γ-(*S*)amino-D-proline

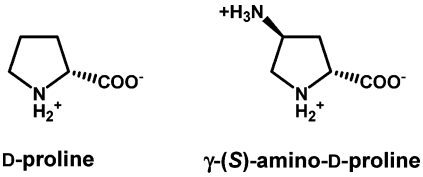

D-proline γ-(*S*)-amino-D-proline

hydrating. Measurements were acquired in two independent preparations with good reproducibility between experiments.

Hydrophobicity by RP-HPLC. Peptides were dissolved in water and injected onto a Vydac C8 reverse-phase column (5 μm, 250 mm × 4 mm) using water containing 0.1% trifluoroacetic acid (TFA) as the A solvent and acetonitrile containing 0.1% TFA as the B solvent. The percent acetonitrile required to elute each peptide was determined using a linear gradient of 10−80% B over 70 min and monitoring absorbance at 220 nm. The assay was repeated several times with good reproducibility.

Binding by Isothermal Titration Calorimetry (ITC). Titrations were performed in a VP−ITC Microcal instrument (Microcal, Northampton, MA) at 30 °C with 10 mM SUVs of DOPC/DOPG (7:3) placed in the calorimeter syringe. The peptide solutions (in 10 mM Hepes, pH 7.4, containing either 140 or 300 mM NaCl) were placed in the cell at a concentration of 25−50 μM. The SUV suspensions were prepared such that they were isoosmotic with the solutions contained in the cell. The volume of each injection of SUV was 3 μL. Data were analyzed with the program Origin v5.0.

RESULTS

Peptide Design and Synthesis. The peptides examined in this study are listed in Table 1 and shown schematically in β-hairpin conformation in Figure 1B. The nomenclature of these sequences is modified from that used in our initial report (*13*). Analogues of PG-1 are designated by a five-letter abbreviation that corresponds to the identities of the residues (in order) at positions 6, 8, 10, 13, and 15, with lowercase letters indicating residues with D-chirality. An amino-functionalized D-proline residue (γ-(*S*)amino-D-proline, shown in Chart 3 and prepared as reported in ref 13) is indicated by p*. Thus, TTpTT designates the PG-1 analogue with threonine in place of cysteine at positions 6, 8, 13, and 15, and D-proline in place of arginine at position 10.

In analogue TTpTT, the four cysteines of PG-1 are replaced with threonine, a residue that has a strong intrinsic propensity for β-sheet secondary structure (*40*−*43*). In addition, a D-proline residue is incorporated at the $i + 1$ position of the β-hairpin turn. We (*44*, *45*) and others (*46*, *47*) have shown that placement of D-proline at the β-turn $i + 1$ position in designed peptides greatly stabilizes β-hairpin conformations by promoting type I′ and type II′ β-turns. TTpTT was previously examined by NMR and found to adopt a β-hairpin conformation in aqueous solution (*13*). TTp*TT contains the aminofunctionalized D-proline residue (see Chart 1) at the $i + 1$ position. This single variation, relative to TTpTT, places an additional charge in the turn region of the β-hairpin conformation. PG-1 contains three arginine residues at the turn (positions 9−11), and studies with PG-1 sequence variants have shown that at least two of these three charges are required for antimicrobial activity (*8*). We previously found that replacement of D-proline with γ-(*S*)amino-D-proline causes only moderate effects on antimicrobial activity (*13*). In the current study, we determined whether this additional charge affects peptide−lipid interactions or membrane selectivity.

CTpTC is similar to TTpTT in sequence and charge, but CTpTC is expected to adopt a more rigid conformation because of the internal disulfide; other single-disulfide analogues of PG-1 have previously been reported to display high antimicrobial activity (*9*). TTPTT is a diastereomer of TTpTT that differs only in the chirality of the proline residue at position 10 (the $i + 1$ position of the β-turn). We have shown in several designed peptides that replacing a D-proline residue at the $i + 1$ position of a β-turn with L-proline abolishes β-hairpin folding (*44*, *45*, *48*, *49*). This difference in conformational stability between peptide diastereosomers results from the incompatibility of the local left-handed twist of an L-proline-containing turn and the intrinsic right-handed twist of β-strands (*50*). For peptides that contain D-proline, the enforced geometry of the turn is compatible with a β-strand twist, and therefore, these D-proline-containing turns promote β-hairpin formation. Our earlier work with TTpTT and TTPTT indicates that, as expected, TTpTT displays antimicrobial activity, but TTPTT does not (*13*). Furthermore, we demonstrated that TTpTT adopts a β-hairpin conformation in solution. Our series of PG-1 analogues, which are very similar in sequence but very different in expected conformational behavior, allows us to examine the effects of variable β-hairpin propensity on biological activity and lipid bilayer interactions independent of major alterations in side chain identity.

Structural Analysis by NMR. We sought to determine whether our series of designed analogues displayed the expected conformational behavior. Thus, we conducted structural analysis of selected peptides by ^{1}H NMR. The chemical shift of α-protons in peptides and proteins is sensitive to local secondary structure (*31*, *51*, *52*). The α-protons for residues in β-sheet secondary structure are typically downfield-shifted relative to residues in the random coil state; those in helical secondary structure are shifted upfield. We have shown that these chemical shift measurements may be used to quantify β-hairpin populations (*53*). We previously reported that TTpTT forms a weak β-hairpin in aqueous solution, as judged by downfield α-proton chemical shifts and by NOEs between residues on opposite strands (*13*). Our initial attempt to compare β-hairpin stabilities by α-proton chemical shifts among PG-1, TTpTT, and a quadruple Thr → Ala mutant of TTpTT (sequence + NH_3RGGRLAYARpRFAVAVGR−amide) was hindered by sequence variation among these peptides. Here, we examine CTpTC and TTPTT by NMR and compare them to TTpTT (previously reported) to gain insight into relative β-hairpin populations and the relationship between β-hairpin folding and antimicrobial activity. These three peptides are very similar in sequence; therefore, comparisons of α-proton chemical shifts among them should be readily interpreted in terms of the extent of folding.

The α-proton chemical shift deviations from tabulated random values for core regions (Leu_5 through Val_{16}) of CTpTC and TTPTT are shown in Figure 2 (for comparison, previously reported values for TTpTT are included). As expected, CTpTC displays large α-proton chemical shift deviations from random coil values ($\Delta\delta H_\alpha$), indicating a high

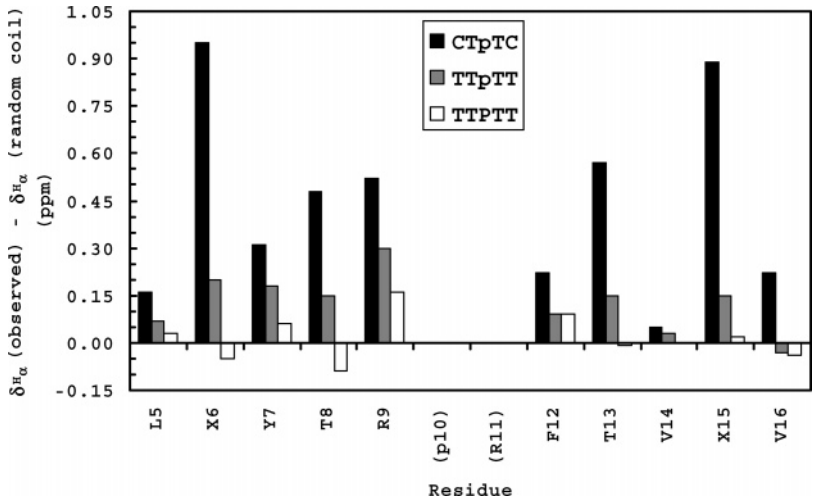

FIGURE 2: α-Proton chemical shift deviation from tabulated random coil values (ref 30) for the core region of CTpTC, TTpTT, and TTPTT. The data for TTpTT were originally published in ref 13. Data were acquired in 9:1 H_2O/D_2O containing 40 mM CD_3COOD/CD_3COONa, pH 3.8 (uncorrected).

β-hairpin content. Generally, three residues in a row with $\Delta\delta H_\alpha > 0.1$ ppm are considered evidence of significant β-sheet structure (*31*). All $\Delta\delta H_\alpha$ values in CTpTC are > 0.1 ppm for the core residues except for that of Val_{14}. We ascribe the smaller $\Delta\delta H_\alpha$ of Val_{14} to anisotropy effects from the aromatic side chain of Tyr_7, which would lie directly across from Val_{14} in the β-hairpin conformation. Similar effects have been observed in PG-1 itself (*6*, *7*, *13*). In contrast, $\Delta\delta H_\alpha$ values for TTPTT are small and randomly distributed about zero, indicating that this peptide is not structured in solution, as expected. Values for TTpTT fall between those of CTpTC and TTPTT. For most residues that are identical among these three peptides (Tyr_7-Arg_9 and Phe_{12}-Val_{14}), the values for TTpTT are closer to those of TTPTT than to those of CTpTC. This observation implies that TTpTT, although not completely unstructured, has only modest β-hairpin stability.

Antimicrobial Activity. We previously reported that PG-1 analogues that contain a single-disulfide constraint retain their antimicrobial potency when 150 mM NaCl is added to the growth media (*13*), which is comparable to results reported earlier by Harwig et al. for other single-disulfide PG-1 analogues (*9*). We sought to determine whether the antimicrobial activity of our designed peptides would be further diminished at a higher salt concentration (300 mM NaCl). In addition, we wanted to examine whether variations in conformational stability between PG-1 and CTpTC (due to the additional disulfide bond in PG-1) would result in losses of activity at these elevated NaCl concentrations. The MIC data for PG-1 and analogues in BHI broth containing an additional 300 mM NaCl are shown in Table 2. For comparison, similar data obtained in BHI (with no additional salt), originally reported in ref 13, are included. PG-1 retained activity in BHI + 300 mM NaCl (differences were within the 2-fold uncertainty of the MIC assay). The linear peptide TTpTT suffers a dramatic loss in activity at the high salt concentration, as does TTp*TT. The single-disulfide-containing CTpTC retained activity in BHI + 300 mM NaCl against most organisms but suffered a substantial loss in potency against *E. faecium* in this medium. These results show that the loss of antimicrobial potentcy for TTpTT and TTp*TT is more dramatic than for CTpTC with increasing NaCl concentrations. CTpTC retains its activity at 150 mM NaCl, but this peptide is partially impaired at 300 mM NaCl. PG-1 is highly resistant to salt-induced inactivation. The differences in salt sensitivity between CTpTC and PG-1 presumably arise from differences in β-hairpin structural stability arising from one disulfide constraint (CTpTC) vs two disulfide constraints (PG-1).

Hemolysis. Many natural antimicrobial peptides display selectivity for disruption of microbial membranes over eukaryotic membranes (*5*). This selectivity is thought to arise from differences in the charge character of the outer leaflet: bacterial membranes contain a higher proportion of negatively charged phospholipids at the extracellular surface than do mammalian membranes. Thus, highly cationic antimicrobial peptides (such as PG-1) are more prone to disrupt bacterial membranes than to disrupt eukaryotic cell membranes because of the higher anionic charge density on the outer leaflet of the former relative to the latter.

In order to determine whether conformational effects in our PG-1 analogue series influence cell-type selectivity, we evaluated PG-1 and the analogues TTpTT, TTp*TT, and CTpTC for the ability to induce human red blood cell lysis (hemolysis; Figure 3). The hemolytic activity of mellitin is shown as a positive control. PG-1 is more hemolytic than the unnatural analogues, with 50% hemolysis (HC50) occurring between 200 and 400 μg/mL. The single-disulfide-containing peptide displays substantial hemolytic activity at higher concentrations (>200 μg/mL); the linear analogues TTpTT and TTp*TT show only minimal (~10%) hemolysis at 400 μg/mL. All β-hairpin-forming peptides are significantly less hemolytic than mellitin (the HC50 for PG-1 is at least 10-fold higher than that for mellitin). Furthermore, the hemolysis induced by the β-hairpin-forming peptides occurs at concentrations several-fold higher than those of the MICs against all bacteria that we examined, indicating that these peptides display high cell-type selectivity. Similar to the antimicrobial activity, the hemolytic activity correlates directly with the β-hairpin-forming propensity among these peptides.

Leakage of Small Molecules from Large Unilamellar Vesicles Promoted by PG-1 and Analogues. Previous reports on PG-1 have suggested that its mechanism of antimicro-

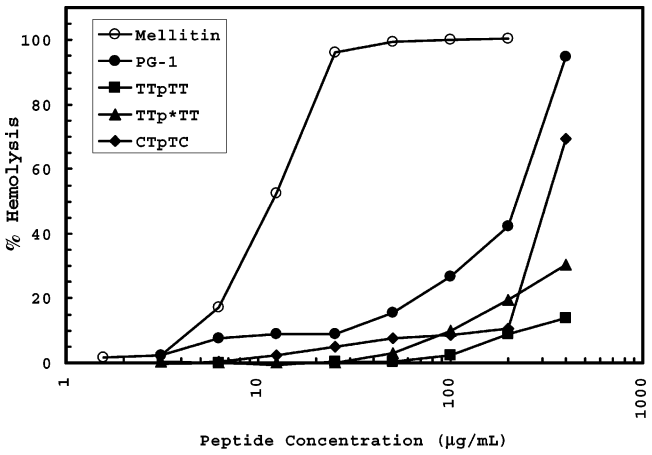

FIGURE 3: Hemolytic activity of PG-1, TTpTT, TTp*TT, and CTpTC. Mellitin was included as a positive control. Peptide concentration was plotted on a logarithmic scale.

bial action involves permeablization of the bacterial membrane (similar to other cationic antimicrobial peptides) (*19*, *20*, *21*). In an effort to investigate the effects of salt and structural rigidity on membrane disruption, we examined the leakage of small molecules from unilamellar vesicles (LUVs) at three different NaCl concentrations using the ANTS/DPX assay (*36*). We prepared LUVs from a 7:3 DOPC/DOPG lipid mixture entrapping ANTS (fluorophore) and DPX (quencher) together in the same vesicle population. Inclusion of DOPG confers a negative charge on the lipid vesicles, which is intended to mimic bacterial cell surfaces. Peptide-induced leakage of ANTS and DPX from the LUVs was detected as an increase in fluorescence that results from the dilution of fluorophore and quencher into the bulk solution.

The peptide-induced leakage of ANTS/DPX from LUVs is shown in Figure 4 as a function of P/L, obtained at a constant lipid concentration of 50 μM with varying concentrations of peptide. In the presence of 50 mM of NaCl, PG-1, TTpTT, TTp*TT, and CTpTC were all able to induce leakage, with comparable potencies (Figure 4A); however, TTPTT induced very little leakage, even at high P/L. Similar studies using a constant peptide concentration of 5 μM and varying amount of lipid gave comparable results (not shown). These leakage data are consistent with the MIC data: PG-1, TTpTT, TTp*TT, and CTpTC manifest potent bacteriostatic activity in BHI broth (low NaCl concentration), but TTPTT does not (*13*).

To determine whether the decreased antimicrobial activity of the linear PG-1 analogues at elevated NaCl concentrations is due to decreased ability of these peptides to promote membrane leakage, we performed additional leakage studies in the presence of 140 or 300 mM NaCl. At 140 mM NaCl, a differentiation among the relative potencies of PG-1 and the D-Pro-containing analogues was observed. PG-1 had the highest potency, followed respectively by CTpTC, TTp*TT, and TTpTT. Analogue TTPTT was again inactive. The relative order of leakage efficiency observed under these conditions correlates well with the bacteriostatic activity in BHI + 150 mM NaCl. At 300 mM NaCl, PG-1 and the single-disulfide-containing analogue CTpTC remained highly active at causing vesicle leakage, but the activity of TTp*TT and TTpTT further declined. These results with LUVs at high salt concentrations match the trends in antimicrobial

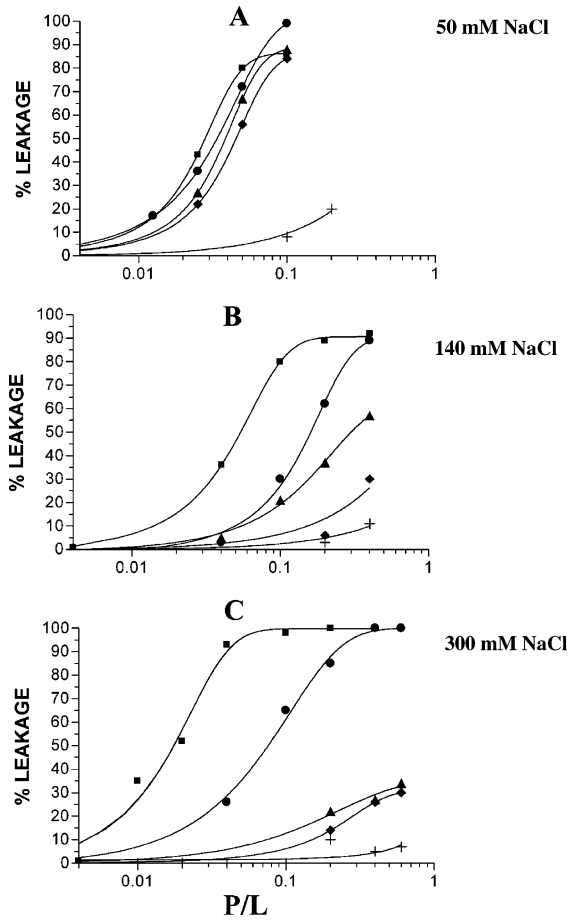

FIGURE 4: Peptide-induced leakage for PG-1 (■), TTpTT (◆), TTp*TT (▲), CTpTC (●), and TTPTT (+) from 7:3 DOPC/DOPG LUVs using the ANTS/DPX assay. The buffer was 10 mM HEPES, 0.1 mM EDTA, pH 7.4 and contained (A) 50 mM NaCl, (B) 140 mM NaCl, or (C) 300 mM NaCl. The LUV concentration was 50 μM.

activities (particularly against *S. aureus* and *E. faecium*), in that the linear analogues lose substantial activity upon addition of 300 mM NaCl to the medium. Some variation in the P/L ratio of induced leakage was observed for PG-1 at different salt concentrations (the reasons for this are not clear, although it is possible that these differences are reflective of the experimental error in the assay). Interestingly, the difference in activity between PG-1 and CTpTC increases from 140 to 300 mM NaCl. These results indicate that CTpTC retains significant leakage-inducing potency at high NaCl concentrations, but this peptide is more sensitive to salt than is PG-1. The excellent correlation between the relative efficiency with which each peptide induces leakage from large unilamellar vesicles and the antimicrobial potencies provides further evidence that the mechanism of bacterial growth inhibition of PG-1 peptides and its analogues involves membrane permeabilization (*9*, *19*, *21*). Furthermore, the loss of ability to induce leakage observed with the linear analogues at elevated salt concentrations suggests that the reduction in antimicrobial potency of these analogues at high NaCl concentrations arises from detrimental effects of the salt on the ability of the peptides to disrupt the membrane barrier.

Leakage of Fluorescence-Labeled Dextran from Large Unilamellar Vesicles Promoted by PG-1 and Analogues. Several models have been proposed for the mechanism of

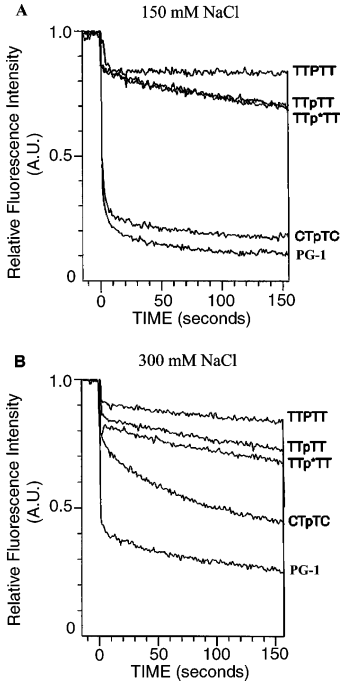

FIGURE 5: Leakage of 10 kDa Oregon Green-labeled dextran from 7:3 DOPC/DOPG LUVs in 10 mM HEPES, 1 mM EDTA, pH 7.4; contained: (A) 150 mM NaCl or (B) 300 mM NaCl. The P/L was 0.1, and the LUV concentration was 50 μM.

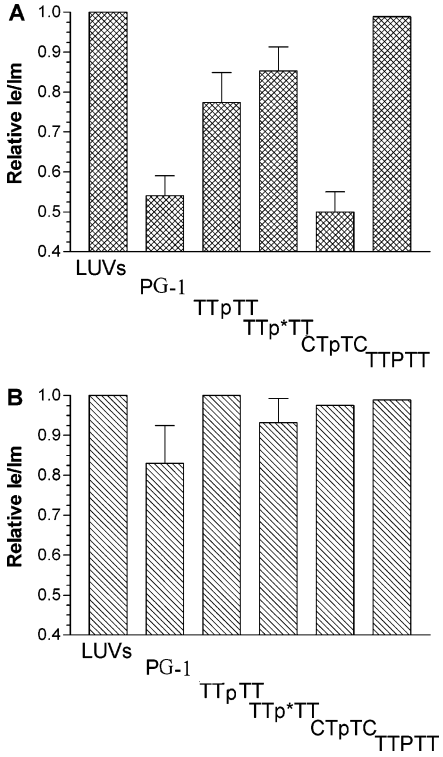

FIGURE 6: Lipid transbilayer flipping ability of PG-1 and analogues against LUVs composed of (A) 7:3 DOPC/DOPG or (B) DOPC only. Experiments were performed at 37 °C with 20 μM LUVs and a P/L of 10.

action of antimicrobial agents (*5*, *54*, *55*). In one model, known as the barrel-stave mechanism, the peptides are proposed to form small, discrete peptide-lined channels in the bacterial membrane. According to a very different mechanism, the carpet model, the peptide solubilizes portions of the membrane by carpeting the bilayer with peptide, forming large openings. Other models include the formation of large peptide-lined pores (toroidal pore) (*5*, *56*) or discoidal lipid−peptide complexes (*19*, *21*). To explore the mechanisms by which PG-1 and our analogues interact with lipid bilayers, we investigated their ability to promote leakage of large dextran molecules (10 kDa) from 7:3 DOPC/DOPG vesicles at 150 and 300 mM NaCl (Figure 5). (Experiments of this type could not be performed at low (<50 mM) NaCl concentrations because of vesicle collapse.)

At 150 mM NaCl, the trends in 10 kDa dextran leakage were similar to those observed with the smaller ANTS/DPX molecules: PG-1 and CTpTC showed a strong ability to induce leakage, TTpTT and TTp*TT were less active, and TTPTT was inactive. At 300 mM NaCl, release of dextran was generally slower than at lower NaCl concentrations, suggesting that the efficiency of large-scale membrane disruption is attenuated at higher NaCl concentrations. PG-1 again was the most active at these high salt concentrations, followed respectively by CTpTC, TTp*TT, and TTpTT. This activity order is consistent with the order of antimicrobial activities at 300 mM NaCl. These results demonstrate that both PG-1 and CTpTC are able to form membrane pores at least 3−4 nm in diameter at high salt concentration and are consistent with the hypothesis that PG-1 and its analogues function by membrane disruption. However, these results alone do not allow us to distinguish among the different models for membrane disruption (carpet, barrel-stave, toroidal pore, or other). Analogues TTpTT and TTp*TT are much less efficient at releasing 10 kDa dextran under these conditions. Analogue TTPTT had no activity even at 150 mM NaCl. These observations suggest that β-hairpin stability has a direct effect on the ability to induce large-scale membrane disruption.

Transbilayer Lipid Diffusion. The efficacy with which antimicrobial peptides induce transbilayer flipping of lipids is frequently used as a measure of the peptides' ability to bind and insert into membranes (*39*, *57*). Lipid flipping is predicted to occur, for example, via the peptide and lipid-lined pore mechanism of Matsuzaki (*59*). Because this process (binding and insertion into the membrane) is critical to peptide-induced membrane disruption, information gained from these types of studies provides insight into the mechanism of antimicrobial activity. Using an assay that measures the peptide-induced dilution of the pyrene probe py-12-PC, we examined the transbilayer lipid diffusion induced by PG-1 and each of the analogues using two different vesicle compositions, 7:3 DOPC/DOPG or DOPC only. The DOPC/DOPG vesicles should be negatively charged and thus are a model for a bacterial membrane. Vesicles composed of the zwitterionic DOPC only should be neutral and are therefore a model of mammalian cell membranes. Examination of the effect of peptides on transbilayer lipid diffusion in vesicles with these two different compositions allows us to gain information on the mechanism of cell-type specificity for PG-1 and its analogues.

As shown in Figure 6A, PG-1 and CTpTC induced considerable transbilayer diffusion with the negatively charged membrane surface (7:3 DOPC/DOPG). Linear analogues TTpTT and TTp*TT showed moderate activity, and TTPTT was inactive. This activity trend matches that of both the antimicrobial assay and the vesicle leakage studies and suggests that the degree of antimicrobial activity is

Table 3: Retention on a C8 RP-HPLC Column

peptide	% B solvent[a]
PG-1	29.4 ± 0.1
CTpTC	27.7 ± 0.2
TTpTT	25.2 ± 0.2
TTPTT	24.8 ± 0.1
TTp*TT	24.4 ± 0.2

[a] The B solvent was acetonitrile containing 0.1% TFA. The data shown are from 3−4 replicates.

directly correlated with a peptide's ability to insert into membranes. Furthermore, the significant degree of transbilayer flipping observed with PG-1 and its analogues is consistent with a toroidal pore or carpet mechanism of membrane disruption (*5*). The barrel-stave mechanism postulates that the peptide molecules lining the small pores do so in well-ordered manner, leaving most of the lipids unperturbed. However, the amount of transbilayer flipping we observe suggests that the membrane disruption induced by PG-1 and its analogues has a pronounced effect on the orientation of lipids in the membrane. Therefore, these results appear to rule out the barrel-stave mechanism.

Figure 6B shows the results with the vesicles consisting of only zwitterionic (i.e., neutral) DOPC lipids. None of the analogues displayed substantial activity except PG-1, which was only moderately able to induce lipid transbilayer diffusion. This result is consistent with the finding that PG-1 exhibits a small amount of hemolytic activity; the other analogues are even less hemolytic. The observed selectivity for the negatively charged vesicles (7:3 DOPC/DOPG) over the neutral vesicles (DOPC only) correlates with the specificity observed in the biological assays (antimicrobial and hemolysis assays) and with other physical studies of PG-1 (*21*). Therefore, these results support the hypothesis that biological specificity among these peptides arises from selectivity in membrane interactions.

Hydrophobicity Analysis via RP-HPLC. Retention time on reverse-phase HPLC columns is frequently used as a measure of peptide hydrophobicity (*58*). Peptides that display hydrophobic side-chain clusters upon formation of secondary structure are retained longer on hydrophobic columns than are similar sequences in which hydrophobic residues are not clustered. In the structure of PG-1, the hydrophobic core residues (Leu_5, Tyr_7, Phe_{12}, Val_{14}, Val_{16}) project from one face of the β-hairpin, giving the molecule an overall amphiphilic character (i.e., distinct hydrophobic and hydrophilic faces) (*6*, *7*). Maintenance of this hydrophobic cluster is important for activity; thus, we reasoned that we could use RP-HPLC as a measure of amphiphilicity and determine whether this parameter correlates with antimicrobial activity. The percent B solvent values (acetonitrile containing 0.1% (v/v) TFA) at which each peptide elutes are listed in Table 3. The rank order of retention on a C8 reverse-phase analytical column matched the order of activity in both the antimicrobial assays and the vesicle leakage studies for PG-1, TTpTT, TTPTT, and CTpTC. However, the differences in retention between the highly potent disulfide bond-containing peptides, CTpTC and PG-1, and TTPTT, which does not have any antimicrobial activity, were small (~5% B solvent difference). This observation suggests that amphiphilicity, as judged by RP-HPLC, is not an accurate predictor of antimicrobial potency or β-hairpin stability. For example, the diastereomers TTpTT and TTPTT show very similar retention behavior despite having drastic differences in antimicrobial activity and significant differences in structural propensity.

Binding by Isothermal Titration Calorimetry (ITC). PG-1 and the analogues CTpTC, TTpTT, and TTp*TT were able to bind DOPC/DOPG (7:3) SUVs in Hepes buffer containing 140 mM NaCl (Figure 7). However, no direct binding to SUVs was observed with TTPTT. At 300 mM NaCl, only the analogues with disulfide bonds (PG-1 and CTpTC) retained the ability to substantially bind to liposomes. PG-1 diplayed higher cooperativity than CTpTC in its binding, suggesting that the rigidity imparted by the second disulfide bond affects liposome binding. Analogues TTpTT and TTp*TT displayed substantial loss of binding capacity at higher salt content. The binding to anionic vesicles in salt was enthalpically driven and the free energy of binding (ΔG) for PG-1 was calculated to be −7.0 kcal/mol, with salt having little effect on ΔG. The binding to anionic vesicles at 300 mM NaCl correlates well with the salt-sensitivity of the antimicrobial activity of these peptides.

DISCUSSION

Correlation of Antimicrobial Activity and Membrane Permeabilization. The order of antimicrobial activity for our set of PG-1-based peptides, CTpTC, TTpTT, and TTPTT, matches closely the order of membrane permeabilization activity observed with lipid vesicles. These results support the hypothesis that the mechanism of antibacterial action for this series of peptides involves disruption of bacterial membranes, as has been proposed previously by others for PG-1 itself (*9*, *19*, *21*). A similar mechanism for antimicrobial activity is postulated for larger β-sheet antimicrobial peptides (e.g., defensins) and α-helical antimicrobial peptides (e.g., magainins) (*5*). Our vesicle leakage studies indicate that PG-1 and its analogues can induce membrane defects of significant size, because both large, fluorophore-conjugated molecules (dextran) and small molecules (ANTX/DPS) are released from liposomes in a peptide-dependent manner. These results suggest that PG-1 and its analogues act on cell membranes through a carpet-like mechanism (*54*, *55;* see also *19* and *21*) or by forming large peptide and lipid-lined pores (i.e., toroidal pores) (*59*). The excellent correlation between the rank order of antimicrobial activity and the rank order of membrane permeabilization ability for the series comprising CTpTC, TTpTT, and TTPTT indicates that any differences in antimicrobial activity among this set of peptides arise from variations in their abilities to cause membrane disruption. Furthermore, these results suggest that the bacterial membrane is the primary or exclusive target for PG-1 and its analogues.

Effects of Conformational Stability on Biological and Physicochemical Activities. The degree of both antimicrobial activity and peptide-induced leakage from liposomes is correlated with the β-hairpin propensity of the peptides as detected by ^{1}H NMR. These results are consistent with our previous observations (*13*), and with those of others (*6*−*10*), which have shown that β-hairpin formation is a key determinant for activity among PG-1 and related β-hairpin peptides. Tam et al. have shown previously that structural rigidification via backbone cyclization in a β-defensin

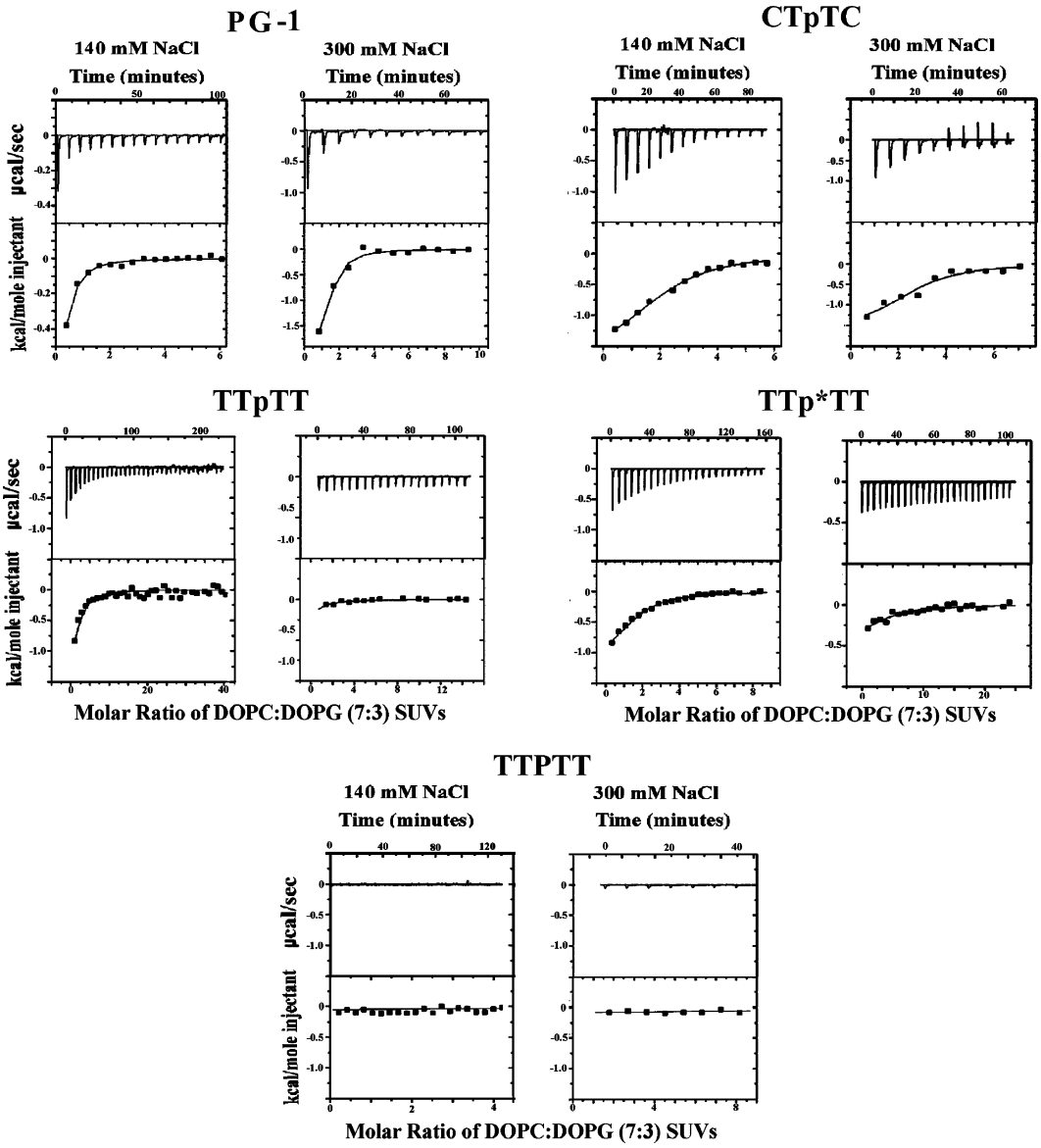

FIGURE 7: ITC titrations at 30 °C in Hepes buffer, pH 7.4. SUVs of DOPC/DOPG (7:3) (10 mM) were placed in the syringe, and 3 μL was injected into 25−50 μM peptides. For each compound presented, the top panel shows the actual titration in μcal/s as a function of time (min) and the bottom panel shows kcal/mol injectant as a function of molar ratio of SUVs; left side panels correspond to 140 mM NaCl and right side panels to 300 mM NaCl.

improves activity, which suggests that conformational propensity has an effect on activity in larger β-sheet antimicrobial peptides (*11*). Parallel work with α-helical peptides has led to conflicting conclusions. Most α-helical antimicrobial peptides must have the ability to form an amphiphilic α-helix in order to retain activity (*58*). However, Oren and Shai have found that peptides containing as many as one-third D-amino acid residues, which are predicted to destabilize α-helical structure, are nonetheless active (*60*). NMR anlysis of a melittin diastereomer containing four D-amino acid residues showed extensive α-helix formation in the presence of micelles (*62*). In contrast, recent NMR analysis of a D-residue-containing peptide shows how such a heterochiral sequence can lead to a globally amphiphilic but nonhelical conformation in the presence of a micelle (*63*).

Origin of Salt Effects. Disulfide-stabilized peptides PG-1 and CTpTC displayed significantly higher resistance to inactivation by high salt concentrations than did linear analogues TTpTT and TTp*TT. Reduced salt sensitivity of disulfide-stabilized peptides was observed also in vesicle permeabilization studies. The tolerance of high salt concentrations by the rigidified peptides suggests that salt-induced inactivation of linear analogues is somehow related to diminished β-hairpin folding propensity. However, we have previously shown that the β-hairpin folding of TTpTT in aqueous solution is not adversely affected by the addition of 150 mM NaCl (*13*). Therefore, any salt-induced conformational effects that lead to inactivation of the linear peptides must be manifested only in the presence of a membrane.

Our observations can be explained as follows. Cell or vesicle disruption requires that the peptide be attracted to the membrane surface. This attraction has a substantial electrostatic component (cationic peptides/anionic surfaces) and should therefore be attenuated as the salt concentration rises because of counterion screening. We propose that affinity for an anionic membrane surface decreases as

β-hairpin stability decreases among the peptide set that includes PG-1 and the analogues discussed here. We further propose that the membrane affinity of PG-1 itself is so high that substantial binding occurs even under the influence of counterion screening; the membrane affinity of a linear analogue such as TTpTT is intrinsically lower and therefore susceptible to sufficient interference from counterion screening to cause diminished antimicrobial and vesicle disruption activities at the NaCl concentrations we explored. This hypothesis would seem to require that electrostatic attraction between the membrane surface and these peptides is higher in the β-hairpin conformation than that in other conformations available to the linear peptides. Affinity could be conformation-dependent because the β-hairpin conformation is more compact and therefore manifests a higher positive charge density relative to open conformations accessible to linear peptides. Alternatively, perhaps the β-hairpin conformation allows a specific spatial matching of peptide cationic groups with anionic groups on the membrane surface. We favor the charge density hypothesis over specific charge matching because the Arg and Lys side chains and anionic lipid headgroups are flexible, and electrostatic interactions are not strongly dependent on interionic distance. The hypothesis outlined here was tested by evaluating the membrane affinities of PG-1 and the analogues we have developed, as a function of NaCl concentration, by isothermal titration calorimetry (ITC). The results, binding to SUVs of DOPC/DOPG (7:3), demonstrated that all peptides used, except TTPTT, bound to lipid at 140 mM NaCl. At 300 mM NaCl, PG-1 bound most strongly, followed by weaker binding of CTpTC. TTPTT, TTp*TT, and TTpTT did not exhibit significant binding at 300 mM NaCl (Figure 7). These results correlate well with the salt sensitivity of the antimicrobial activity of these peptides.

Our results with PG-1 and its analogues offer an interesting comparison with the larger, α-helical pore-forming peptide colicin E1 (*64*, *65*). Cramer and co-workers used fluorescence resonance energy transfer (FRET) analysis with chromophores on either end of the 178-residue colicin E1 peptide to examine the effects of flexibility on pore-forming activity (*64*). These authors found that a high degree of flexibility was required in this case, because formation of the pore requires significant rearrangement of the protein's ten α-helices. Furthermore, increased membrane surface potential resulted in increased rigidity of colicin E1 in the membrane, thereby reducing its pore-forming efficacy. Recently, Yao and Hong studied local conformational effects in colicin E1 by solid-state NMR (*65*). These authors found that, although global flexibility was required for activity, local rigidity (i.e., rigidity of the α-helix secondary structural elements) was critical. Because PG-1 is composed of only a single, secondary structural unit (a β-hairpin), local rigidity of the molecule is the dominant determinant of membrane disruption efficacy. Similar activity studies with peptide series based on α-helical antimicrobial peptides could indicate whether local rigidity is dominant in those cases, too. We have examined the role of secondary structural rigidity in the antibacterial activity of helix-forming oligomers of β-amino acids ("β-peptides"); our evidence suggests that conformational stability does not exert a large effect on antibacterial efficacy (*66*, *67*).

CONCLUSIONS

Our data suggest that the antibacterial effects exerted by PG-1 and related peptides arise from an interplay among conformational stability, affinity for a membrane surface, and the ability to disrupt a lipid bilayer. A set of PG-1 analogues with incrementally varied propensities for β-hairpin folding, which we developed on the basis of fundamental principles of β-sheet design, has proven to be valuable for elucidating the relationships among physicochemical and biological activities and for exploring the ability of high salt concentrations to modulate antibacterial effects. This peptide series should continue to be useful for mechanistic studies.

REFERENCES

1. Gennaro, R. T., and Zanetti, M. (2000) Structural features and biological activities of the cathelicidin-derived antimicrobial peptides, *Biopolymers 55*, 31−49.
2. Dimarcq, J. L., Bulet, P., Hetru, C., and Hoffman, J. (1998) Cysteine-rich antimicrobial peptides in invertebrates, *Biopolymers 47*, 465−477.
3. Kokryakov, V. N., Harwig, S. S. L., Panyutich, E. A., Shevchenko, A. A., Aleshina, G. M., Shamova, O. V., Korneva, H. A., and Lehrer, R. I. (1993) Protegrins: leukocyte antimicrobial peptides that combine features of corticostatic defensins and tachyplesins, *FEBS Lett. 327*, 231−236.
4. Hancock, R. E. W., and Lehrer, R. (1998) Cationic peptides: a new source of antibiotics, *Trends Biotechnol. 16*, 82−88.
5. Zasloff, M. (2002) Antimicrobial peptides of multicellular organisms, *Nature 415*, 389−395.
6. Fahrner, R. L., Dieckmann, T., Harwig, S. S. L., Lehrer, R. I., Eisenberg, D., and Feignon, J. (1996) Solution structure of protegrin-1, a broad-spectrum antimicrobial peptide from porcine leukocytes, *Chem. Biol. 3*, 543−550.
7. Aumelas, A., Mangoni, M., Roumestand, C., Chiche, L., Despaux, E., Grassy, G., Calas, B., and Chacanieu, A. (1996) Synthesis and Solution Structure of the Antimicrobial Peptide Protegrin-1, *Eur. J. Biochem. 237*, 575−583.
8. Chen, J., Falla, T. J., Liu, H., Hurst, M. A., Fujii, C. A., Mosca, D. A., Embree, J. R., Loury, D. J., Radel, P. A., Chang, C. C., Gu, L., and Fiddes, J. C. (2000) Development of protegrins for the treatment and prevention of oral mucositis: Structure-activity relationships of synthetic protegrin analogues, *Biopolymers 55*, 88−98.
9. Harwig, S. S. L., Waring, A., Yang, H. J., Cho, Y., Tan, L., and Lehrer, R. I. (1996) Intramolecular Disulfide Bonds Enhance the Antimicrobial and Lytic Activities of Protegrins at Physiological Sodium Chloride Concentrations, *Eur. J. Biochem. 240*, 352−357.
10. Mangoni, M. E., Aumelas, A., Charnet, P., Roumestand, C., Chiche, L., Despaux, E., Grassy, G., Calas, B., and Chavanieu, A. (1996) Change in membrane permeability induced by protegrin 1: implication of disulphide bridges for pore formation, *FEBS Lett. 383*, 93−98.
11. Tam, J. P., Chengwei, W., and Yang, J. L. (2000) Membranolytic selectivity of cystine-stabilized cyclic protegrins, *Eur. J. Biochem. 267*, 3289−3300.
12. Mani, R., Waring, A. J., Lehrer, R. I., and Hong, M. (2005) Membrane-Disruptive Abilities of β-Hairpin Antimicrobial Peptides Correlate with Conformation and Activity: A ^{31}P and ^{1}H NMR Study, *Biochim. Biophys. Acta 1716*, 11−18.
13. Lai, J. R., Huck, B. R., Weisblum, B., and Gellman, S. H. (2002) Design of Non-cysteine-containing Antimicrobial β-Hairpins: Structure−Activity Relationship Studies with Linear Protegrin-1 Analogues, *Biochemistry 41*, 12835−12842.
14. Shankaramma, S. C., Athanassiou, Z., Zerbe, O., Moehle, K., Mouton, C., Bernardini, F., Vrijbloed, J. W., Obrecht, D., and Robinson, J. A. (2002) Macrocyclic Hairpin Mimetics of the Cationic Antimicrobial Peptide Protegrin I: A New Family of Broad-Spectrum Antibiotics, *ChemBioChem 3*, 1126−1133.
15. Roumestand, C., Louis, V., Aumelas, A., Grassy, G., Calas, B., and Chavanieu, A. (1998) Oligomerization of protegrin-1 in the presence of DPC micelles. A proton high-resolution NMR study, *FEBS Lett. 421*, 263−267.

16. Sokolov, Y., Mirzabekov, T., Martin, D. W., Lehrer, R. I., and Kagan, B. L. (1999) Membrane channel formation by antimicrobial protegrins, *Biochim. Biophys. Acta 1420*, 23−29.
17. Hill, C. P., Yee, J., Selsted, M. E., and Eisenberg, D. (1991) Crystal structure of defensin HNP-3, an amphiphilic dimer: mechanisms of membrane permeabilization, *Science 251*, 1481−1485.
18. Yang, L., Weiss, T. M., Lehrer, R. I., and Huang, H. W. (2000) Crystallization of Antimicrobial Pores in Membranes: Magainin and Protegrin, *Biophys. J. 79*, 2002−2009.
19. Yamaguchi, S., Hong, T., Waring, A., Lehrer, R. I., and Hong, M. (2002) Solid-State NMR Investigations of Peptide−Lipid Interaction and Orientation of a β-Sheet Antimicrobial Peptide, Protegrin, *Biochemistry 41*, 9852−9862.
20. Heller, W. T., Waring, A. J., Lehrer, R. I., and Huang, H. W. (1998) Multiple States of β-Sheet Peptide Protegrin in Lipid Bilayers, *Biochemistry 37*, 17331−17338.
21. Gidalevitz, D., Ishitsuki, Y., Muresan, A. S., Konovalov, O., Waring, A. J., Lehrer, R. I., and Lee, K. Y. (2003) Interaction of antimicrobial peptide protegrin with biomembranes, *Proc. Natl. Acad. Sci. U.S.A. 27*, 6302−6307.
22. Goldman, M. J., Anderson, G. M., Stolzenberg, E. D., Kari, U. P., Zasloff, M., and Wilson, J. M. (1997) Human β-Defensin-1 Is a Salt-Sensitive Antibiotic in Lung That Is Inactivated in Cystic Fibrosis, *Cell 88*, 553−560.
23. Smith, J. J., Travis, S. M., Greenberg, Ep. P., and Welsh, P. J. (1996) Cystic Fibrosis Airway Epithelia Fail to Kill Bacteria Because of Abnormal Airway Surface Fluid, *Cell 85*, 229−236.
24. Yu, Q., Lehrer, R. I., and Tam, J. P. (2000) Engineered Salt-Insensitive-Defensins with End-to-End Circularized Structures, *J. Biol. Chem. 275*, 3943−3949.
25. Schibli, D. J., Hunter, H. N., Aseyev, V., Starner, T. D., Wiencek, J. M., McCray, P. B., Jr., Tack, B. F., and Vogel, H. J. (2002) The Solution Structures of the Human β-Defensins Lead to a Better Understanding of the Potent Bactericidal Activity of HBD3 against *Staphylococcus aureus*, *J. Biol. Chem. 277*, 8279−8289.
26. Mosca, D. A., Hurst, M. A., So, W., Viajar, B. S. C., Fujii, C. A., and Falla, T. J. (2000) IB-367, a Protegrin Peptide with In Vitro and In Vivo Activities against the Microflora Associated with Oral Mucositis, *Antimicrob. Agents Chemother. 44*, 1803−1808.
27. Piotto, M., Saudek, V., and Sklenar, V. (1992) Gradient-tailored excitation for single-quantum NMR-spectroscopy of aqueous-solutions. *J. Biomol. NMR 2*, 661−665.
28. Bax, A., and Davis, D. G. (1985) MLEV-17-Based two-dimensional homonuclear magnetization transfer spectroscopy, *J. Magn. Reson. 65*, 355−360.
29. Bothner-By, A. A., Stephens, R. L., Lee, J., Warren, C. D., and Jeanloz, R. W. (1984) Structure determination of a tetrasaccharide: transient nuclear Overhauser effects in the rotating frame, *J. Am. Chem. Soc. 106*, 811−813.
30. Jeener, J., Meier, B. H., Bachmann, P., and Ernest, R. R. (1979) Investigation of exchange processes by two-dimensional NMR spectroscopy, *J. Chem. Phys. 71*, 4546−4553.
31. Wuthrich, K. (1986) *NMR of Proteins and Nucleic Acids*, Wiley, New York.
32. Yanisch-Perron, C., Viera, J., and Messing, J. (1985) Improved M13 phage cloning vectors and host strains: nucleotide sequences of the M13mpl8 and pUC19 vectors, *Gene 33*, 103−119.
33. Young, F. E., Smith, C., and Reilly, B. E. (1969) Chromosomal Location of Genes Regulating Resistance to Bacteriophage in *Bacillus subtilis*, *J. Bacteriol. 98*, 1087−1097.
34. Weisblum, B., and Demohn, V. (1969) Erythromycin-Inducible Resistance in *Staphylococcus aureus:* Survey of Antibiotic Classes Involved, *J. Bacteriol. 98*, 447−452.
35. Nicas, T. I., Wu, C. Y. E., Hobbs, J. N., Preston, D. A., and Allen, N. E. (1989) Characterization of vancomycin resistance in *Enterococcus faecium* and *Enterococcus faecalis*, *Antimicrob. Agents Chemother. 33*, 1121−1124.
36. Ellens, H., Bentz, J., and Szoka, F. C. (1985) Proton- and calcium-induced fusion and destabilization of liposomes, *Biochemistry 24*, 3099−3106.
37. Ames, B. N. (1966) Assay of Inorganic Phosphate, Total Phosphate and Phosphatases, *Methods Enzymol. 8*, 115−118.
38. Sharpe, J. C., and London, E. (1999) Diphtheria Toxin Forms Pores of Different Sizes Depending on Its Concentration in Membranes: Probable Relationship to Oligomerization, *J. Membr. Biol. 171*, 209−221.
39. Muller, P., Schiller, S., Wieprecht, T., Dathe, M., and Herrmann, A. (2000) Continuous measurement of rapid transbilayer movement of a pyrene-labeled phospholipids analogue, *Chem. Phys. Lipids 106*, 89−99.
40. Chou, P. Y., and Fasman, G. D. (1974) Conformational parameters for amino acids in helical, β-sheet, and random coil regions calculated from proteins, *Biochemistry 13*, 211−245.
41. Chou, P. Y., and Fasman, G. D. (1978) Empirical Predictions of Protein Conformation, *Annu. Rev. Biochem. 47*, 251−276.
42. Kim, C. A., and Berg, J. N. (1993) Thermodynamic β-sheet propensities measured using a zinc-finger host peptide, *Nature 362*, 267−270.
43. Minor, D. L., Jr., and Kim, P. S. (1994) Measurement of the β-sheet-forming propensities of amino acids, *Nature 367*, 660−663.
44. Haque, T. S., Little, J. C., and Gellman, S. H. (1997) Stereochemical Requirements for β-Hairpin Formation: Model Studies with Four-Residue Peptides and Depsipeptides, *J. Am. Chem. Soc. 118*, 6975−6985.
45. Haque, T. S., and Gellman, S. H. (1997) Insights on β-Hairpin Stability in Aqueous Solution from Peptides with Enforced Type I′ and Type II′ β-Turns, *J. Am. Chem. Soc. 119*, 2303−2304.
46. Shankaramma, S. C., Moehle, K., James, S., Vrijbloed, J. W., Obrecht, D., and Robinson, J. A. (2003) A family of macrocyclic antibiotics with a mixed peptide−peptoid β-hairpin backbone conformation, *Chem. Commun.* 1842−1843.
47. Das, C., Naganadowda, G. A., Karle, I. L., and Balaram, P. (2001) Designed β-hairpin peptides with defined tight turn stereochemistry, *Biopolymers 58*, 335−346.
48. Stanger, H. E., and Gellman, S. H. (1998) Rules for Antiparallel β-Sheet Design: D-Pro-Gly Is Superior to L-Asn-Gly for β-Hairpin Nucleation, *J. Am. Chem. Soc. 120*, 4236−4237.
49. Gellman, S. H. (1998) Minimal model systems for β-sheet secondary structure in proteins, *Curr. Opin. Chem. Biol. 2*, 717−725.
50. Salemme, F. R. (1983) Structural Properties of Protein β-sheets, *Prog. Biophys. Mol. Biol. 92*, 95−133.
51. Wishart, D. S., Sykes, B. D., and Richards, F. M. (1991) Relationship between nuclear magnetic resonance chemical shift and protein secondary structure, *J. Mol. Biol. 222*, 311−333.
52. Wishart, D. S., Sykes, B. D., and Richards, F. M. (1992) *Biochemistry 31*, 1647−1651.
53. Syud, F. A., Espinosa, J. F., and Gellman, S. H. (1999) NMR-Based Quantification of β-Sheet Populations in Aqueous Solution through Use of Reference Peptides for the Folded and Unfolded States, *J. Am. Chem. Soc. 121*, 11577−11578.
54. Shai, Y. (1999) Mechanism of the Binding, Insertion, and Destabilization of Phospholipid Bilayer Membranes by α-Helical Antimicrobial and Cell Non-Selective Membrane-Lytic Peptides, *Biochim. Biophys. Acta Biomembranes 1462*, 55−70.
55. Oren, Z., and Shai, Y. (1998) Mode of Action of Linear Amphipathic α-Helical Antimicrobial Peptides, *Biopolymers 47*, 451−463.
56. Epand, R. F., Martinou, J. C., Montessuit, S., and Epand, R. M. (2003) Transbilayer Lipid Diffusion Promoted by Bax: Implications for Apoptosis, *Biochemistry 42*, 14576−14582.
57. Blondelle, S. E., Houghten, and R. A. (1992) Design of model amphipathic peptides having potent antimicrobial activities, *Biochemistry 31*, 12688−12694.
58. Tossi, A., Sandri, L., and Giangaspero, A. (2000) Amphipathic, -helical antimicrobial peptides, *Biopolymers 55*, 4−30.
59. Matsuzaki, K. (1998) Magainins as Paradigm for the Mode of Action of Pore-Forming Polypeptides, *Biochim. Biophys. Acta 1376*, 391−400.
60. Oren, Z., and Shai, Y. (2000) Cyclization of a Cytolytic Amphipathic -Helical Peptide and Its Diastereomer: Effect on Structure, Interaction with Model Membranes, and Biological Function, *Biochemistry 39*, 6103−6114.
61. Li, X., Li, Y., Han, H., Miller, D. W., and Wang, G. (2006) Solution Structures of Human LL-37 Fragments and NMR-Based Identification of a Minimal Membrane-Targeting Antimicrobial Peptide and Anticancer Region, *J. Am. Chem. Soc. 128*, 5776−5785.
62. Sharon, M., Oren, Z., Shai, Y., and Anglister, J. (1999) 2D-NMR and ATR-FTIR Study of the Structure of a Cell-Selective Diastereomer of Melittin and its Orientation in Phospholipids, *Biochemistry 38*, 15305−15316.
63. Li, X., Li, Y., Han, H., Miller, D. W., and Wang, G. (2006) Solution Structures of Human LL-37 Fragments and NMR-Based Identification of a Minimal Membrane-Targeting Antimicrobial

Peptide and Anticancer Region, *J. Am. Chem. Soc. 128*, 5776−5785.
64. Zakharov, S. D., Rokiskaya, T. I., Shapovalov, V. L., Antonenko, Y. N., and Cramer, W. A. (2002) Tuning the Membrane Surface Potential for Efficient Toxin Import, *Proc. Natl. Acad. Sci. U.S.A. 99*, 8654−8659.
65. Yao, X. L., and Hong, M. (2006) Effects of Anionic Lipid and Ion Concentrations on the Topology and Semental Mobility of Colicin Ia Channel Domain from Solid-State NMR, *Biochemistry 45*, 289−295.
66. Raguse, T. R., Porter, E. A., Weisblum, B., and Gellman, S. H. (2002) Structure−Activity Studies of 14-Helical Antimicrobial β-Peptides: Probing the Relationship Between Conformational Stability and Antimicrobial Potency, *J. Am. Chem. Soc. 124*, 12774−12785.
67. Epand, R. F., Raguse, T. L., Gellman, S. H., and Epand, R. M. Antimicrobial 14-Helical β-Peptides: Potent Bilayer Disrupting Agents, *Biochemistry 43*, 9527-9535.

BI0617759